

IAC-21-D2.6.1

**Towards a Reusable First Stage Demonstrator:  
CALLISTO – Technical Progresses & Challenges**

**Sven Krummen<sup>a,\*</sup>, Jean Desmariaux<sup>b</sup>, Saito Yasuhiro<sup>c</sup>,  
Marcelo Boldt<sup>a</sup>, Lâle Evrim Briese<sup>a</sup>, Nathalie Cesco<sup>b</sup>, Christophe Chavagnac<sup>b</sup>, Elisa Cliquet Moreno<sup>b</sup>,  
Etienne Dumont<sup>a</sup>, Tobias Ecker<sup>a</sup>, Silas Eichel<sup>a</sup>, Moritz Ertl<sup>a</sup>, Sofia Giagkozoglou Vincenzino<sup>a</sup>, Thilo Glaser<sup>a</sup>,  
Christian Grimm<sup>a</sup>, Michel Illig<sup>b</sup>, Shinji Ishimoto<sup>c</sup>, Josef Klevanski<sup>a</sup>, Norbert Lidon<sup>b</sup>, Olaf Mierheim<sup>a</sup>,  
Jean-François Niccolai<sup>b</sup>, Siebo Reershemius<sup>a</sup>, Bodo Reimann<sup>a</sup>, Johannes Riehmer<sup>a</sup>, Marco Sagliano<sup>a</sup>,  
Henning Scheufler<sup>a</sup>, Anton Schneider<sup>a</sup>, Silvio Schröder<sup>a</sup>, René Schwarz<sup>a</sup>, David Seelbinder<sup>a</sup>, Malte Stief<sup>a</sup>,  
Jens Windelberg<sup>a</sup>, Svenja Woicke<sup>a</sup>**

<sup>a</sup> *Deutsches Zentrum fuer Luft- und Raumfahrt e.V. (DLR), Germany*

<sup>b</sup> *Centre National d' Etudes Spatiales (CNES), France*

<sup>c</sup> *Japan Aerospace Exploration Agency (JAXA), Japan*

\* Corresponding Author

**Abstract**

In order to investigate the capabilities of a reusable launch system, JAXA, CNES and DLR have jointly initiated the project CALLISTO (“Cooperative Action Leading to Launcher Innovation for Stage Toss-back Operations”). The goal of this cooperation is to launch, recover and reuse a first stage demonstrator to increase the maturity of technologies necessary for future operational reusable launch vehicles (RLV) and to build up know-how on such vehicles under operational and developmental aspects.

As the project has now turned into the detailed design phase, significant technical progresses have been made in definition, analysis and testing of systems and subsystems. The CALLISTO vehicle itself constitutes a subscale vertical take-off vertical landing (VTVL) stage with an overall length of 13.5 m and a take-off mass of less than 4 tons, which is propelled by a throttleable LOX/LH2 engine. It is capable to perform up to 10 consecutive flights during the planned flight campaign in French Guiana. Globally, the development effort on this system is equally shared between the three project partners.

This paper presents the recent achievements in development of the key technologies for the reusable launch vehicle. While the design of critical subsystems has reached PDR level, detailed analyses and first breadboard tests have been performed successfully. These results are presented and discussed within the perimeter of the CALLISTO development roadmap. Possible technical challenges are indicated and their resolution methods are examined. Finally, the upcoming development steps are described which are foreseen to move forward to the qualification and maiden flight campaign.

**Keywords:** CALLISTO, reusable launch vehicle (RLV), vertical take-off vertical landing (VTVL)

**Abbreviations**

AEDB – Aerodynamic Data Base

ALS – Approach and Landing System

ATDB – Aerothermal Data Base

AVF – Avionics Validation Facility

CALLISTO – Cooperative Action Leading to Launcher Innovation for Stage Toss-back Operations

CDR – Critical Design Review

CFD – Computational Fluid Dynamics

CFRP – Carbon Fiber Reinforced Polymers

CSG – French Guiana European Spaceport

CSTB – Scientific and Technical Center for Building

DC – Direct Current

DLM – Doublet Lattice Method

DNW – German-Dutch Wind Tunnels

ELV – Expendable Launch Vehicle

EMC – Electro-Magnetic Compatibility

FCS/A – Aerodynamic Control System

FCS/R – Reaction Control System

FCS/V – Thrust Vector Control System

FEM – Finite Element Model

FNS – Flight Neutralization System

FRR – Flight Readiness Review

GNSS – Global Navigation Satellite System

GSE – Ground Support Equipment

HNS – Hybrid Navigation System

HST – High-Speed Tunnel, DNW

IMU – Inertial Measurement Unit

LAMA – Landing & Mobility Test Facility, DLR

LH2 – Liquid Hydrogen

LLRM – Launch Lock Release Mechanism

LOX – Liquid Oxygen

MECO – Main Engine Cut-Off

M&RO – Maintenance & Repair Operations

NTC – Noshiro Rocket Testing Center, JAXA  
 PDR – Preliminary Design Review  
 ReFEx – Reusable Flight Experiment  
 RLV – Reusable Launch Vehicle  
 RSR – Reusable Sounding Rocket  
 RTK – Real-Time Kinematic  
 RV-X – Reusable Vehicle Experiment  
 TMK – Trisonic Wind Tunnel, DLR  
 VEB – Vehicle Equipment Bay  
 VPH – Vehicle Preparation Hall  
 VTHL – Vertical Take-off Horizontal Landing  
 VTVL – Vertical Take-off Vertical Landing  
 WTT – Wind Tunnel Test

## 1. Introduction

During the last years significant changes in the space transportation market could be observed: While the amount of commercial and institutional payloads has noticeably increased, launch providers tried to reduce their service cost by introducing new technologies to stay competitive. In this environment reusable launch vehicles (RLV), as they are operated e.g. by SpaceX, have emerged as highly cost-efficient alternatives to conventional expendable launch vehicles (ELV), also giving additional operational flexibility to serve a broad range of payloads and missions.

The national space centers DLR, CNES and JAXA have recognized this development and shared the common vision to increase the maturity of key technologies for future operational RLVs. Therefore, in 2017 the trilateral CALLISTO project has been jointly initiated to develop, launch, recover and reuse a vertical take-off and vertical landing (VTVL) rocket stage demonstrator. The maiden flight is planned in 2024.

The main goal of CALLISTO is to build up know-how on VTVL first stages under operational and developmental aspects. Particularly, data shall be gathered under representative conditions during flight, but also during development and refurbishment phases, to better assess advantages and drawbacks of such vehicles. This knowledge will support the design of next generation launch vehicles in Japan and Europe, like the successors of H3 or Ariane 6. [1][2]

## 2. System Overview

The CALLISTO system includes the demonstrator vehicle itself, its ground segment, and its set of flight experiments.

The vehicle is a 13.5m long VTVL stage, with an external diameter of 1100mm and a maximum take-off mass of less than 4 tons. It is propelled by a 40kN class LOX/LH2 engine with a throttling capability from 115% down to 40%. [3]

From a geometric standpoint, the vehicle is divided into six modules, each composed of a primary structure with attached equipment. These vehicle modules are:

- Nose Fairing Module, ensuring the relevant nose aeroshape at ascent and protecting the housed GNSS antenna and elements of the Flight Neutralization System (FNS);
- Vehicle Equipment Bay Module (VEB), accommodating the Reaction Control System (FCS/R), four deployable Control Aerosurfaces (FCS/A) as well as avionics and FNS items;
- LOX Tank Module, and below, LH2 Tank Module, whose primary structures are the load-carrying LOX and LH2 propellant tanks, and accommodating the main part of the two cable ducts traveling along the vehicle side;
- Bottom Module, housing in particular the engine, the thrust vector control (FCS/V) and the tank pressurization system, as well as some avionics and fluidics items;
- Approach and Landing System (ALS), which is composed of four landing legs attached to the Bottom Module. A dedicated pneumatic system is housed inside the Bottom Module.

As the project partners decided to operate the vehicle from the French Guiana European Spaceport (CSG) a devoted Launch Complex has also to be developed. Since the CSG is home for different launch systems, the CALLISTO Launch Complex\* has to friendly interface with the Launch Range and its operating rules, including safety limitations.

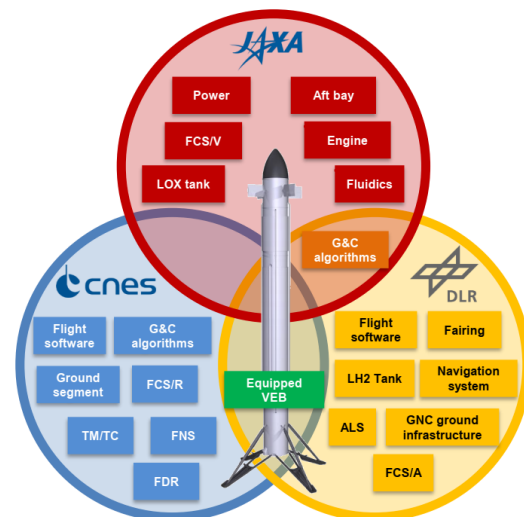


Figure 1: Set of CALLISTO's major subsystems, arranged by the workshare between project partners

\* Each launcher operated in CSG benefits from its own installations and its Ground Support Equipment (GSE): the Launch Complex. Besides that, there are installations and GSEs used by the CSG Launch Range for supporting the different launcher programs and their operations: primary resource distribution (e.g. electricity, water), weather forecast, launcher motion tracking, etc.

### 3. Development of System and Subsystems

The project has now turned into the detailed design phase with numerous progresses in definition, analysis and testing of CALLISTO system and its subsystems. A breakdown of the primary products and workshare in between project partners is provided in Figure 1.

The following paragraphs will present some recent achievements in development of selected key technologies and also discuss challenges that have been observed during detailed design.

#### 3.1 Mission Design

CALLISTO's mission design is based on its flight test plan which targets an in-flight system validation, since some technologies cannot be tested in a representative environment on ground, as well as a progressive exploration of the flight envelope, to mitigate risks during the flight campaign. According to these principles the mission design has now converged towards two main categories of missions:

- Low energy flights, which will keep the engine running in a steady state while providing large margins in the propellant budget;
- High energy flights, which will either switch the engine to "Idle mode" or perform a main engine cut-off (MECO) in flight. Along the flight envelope increase, propellant reserves will be lowered to gradually extend the descent flight domain.

Another key driver for mission design is the touchdown strategy at landing. While first flights are planned to perform the touchdown phase with the engine still running, high energy flights will feature a MECO above ground. This necessitates a higher accuracy to achieve touchdown conditions compatible with vehicle design limits.

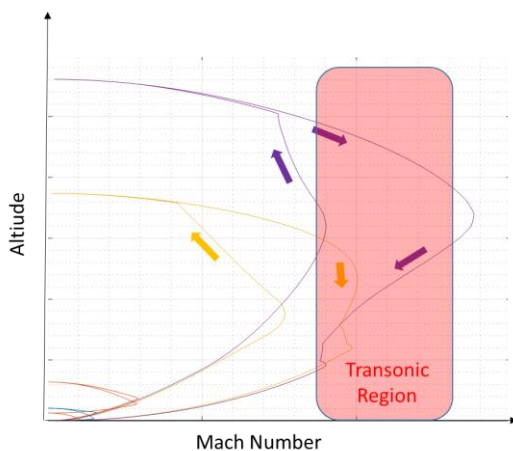


Figure 2: Incremental increase of the flight envelope, from low-risk to high-energy flights

A notional view of incremental increase of the flight envelope is provided in Figure 2. At the bottom left low energy flights are depicted which feature velocities below Mach 0.3 and a relatively low altitude. In contrast on the right, high energy flights will reach the transonic regime and beyond.

#### 3.2 Rocket Propulsion System

##### 3.2.1 Engine

In previous research activity JAXA developed the experimental Reusable Sounding Rocket engine (RSR), which is generating 40kN thrust at sea level and demonstrated reusability over more than 100 times [4]. It is currently used for the Japanese Reusable Vehicle Experiment (RV-X), which finished final stage firing tests in September 2021 and the final preparation for the flight test in March 2022.

The engine for CALLISTO is equivalent to the RSR engine, but JAXA will redesign and newly manufacture an improved version, called RSR2. An overview of this engine is shown in Figure 3. Due to these improvements, the thrust of the RSR2 engine is increased by 15%, while the mass and envelope are reduced to fit the CALLISTO vehicle.

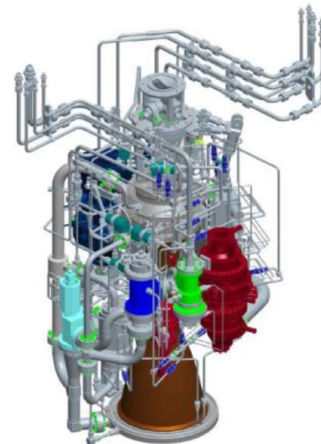


Figure 3: Architecture of the RSR2 Engine

In addition to reusability, these engines have throttling and re-ignition capabilities as distinguished characteristics. The RSR2 engine can modulate its thrust continuously between 16kN and 46kN under sea level conditions.

##### 3.2.2 Liquid Oxygen Tank

JAXA is also developing the LOX tank as depicted in Figure 4. The LOX tank is situated between the LH2 tank on its bottom interface and the VEB structure on its top interface. Both interfaces are designed as L-flanges. In addition, the LOX Tank is interfacing with numerous further products such as the cable ducts and related fluidics products, like valves and fluidic lines.



Figure 4: Geometry of the LOX Tank

The characteristics of this newly developed tank are the equipped propellant management devices and a welding-free structure. The former characteristics allow the investigation of fluid motion during appropriate attitude change maneuvers in flight, to demonstrate the feasibility of reusable first stages. Besides that, the welding-free mechanical connections between the tank cylinder, the domes and the interface rings avoid interference with the production schedule of other vehicle to shorten the development schedule.

### 3.2.3 Liquid Hydrogen Tank

The LH2 tank is the largest module of the CALLISTO vehicle. It is located between the aft-bay and the LOX tank, having a total length of about 6m. The tank uses an integral structural design based on seven aluminum alloy segments with different wall thicknesses.

The structure of the LH2 tank must be able to withstand a challenging combination of global and local loads during launch, while still serving as a vessel for the liquid propellant. Same as for the entire vehicle, optimization of mass is an essential issue for the structural design. The main design driver is here the prevention of buckling for different tank pressurization conditions and phases in the operational life cycle, besides few handling and manufacturing constraints.

One of the sizing load cases is during ground phases when the LH2 tank is unpressurized and the CALLISTO vehicle is either verticalized and supported by the launch table or on its legs. For this load case a dedicated finite element model has been developed which includes all major structures of the vehicle. This approach was selected to consider effects of force over-fluxes from adjacent structures in the design.

For instance, for the preliminary sizing of the tank segments two loads were considered: a constant axial force representing the mass of the modules above the LH2 tank and the lateral wind loads. Here, the wind

loads were simplified as a pressure distribution acting orthogonally on the vehicle's skin, assuming a laminar flow around a cylindrical body of infinite length.

Similar studies have also been performed for the different flight conditions with various tank and ambient pressures. In these studies, additional mechanical loads due to internally and externally attached equipment were considered, such as cable ducts, fluidics equipment and local openings for feed throughs.

Same as for the structural design, the mass budget is an important aspect of the functional design of the LH2 tank, since the resources of available propellant and Helium, as pressurization gas, have to be managed. A sound design of components the anti-vortex device, the pressurization port and the sloshing suppression device, as well as the effectiveness of the overall thermal insulation, are vital for optimizing the usable propellant and minimizing the Helium mass budget.

The effectiveness of baffles inside the tank is studied for the CALLISTO mission profile as shown in Figure 5. One of the key features is to limit the motion of the propellant, while not increasing the free surface area by splashing and droplet formation, to limit the heat and mass transfer between the two propellant phases.

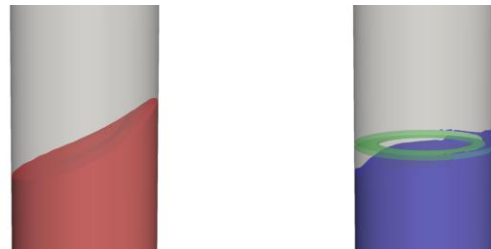


Figure 5: Effectiveness of tank baffles for the CALLISTO mission profile (left: tank without baffle; right: effective sloshing suppression).

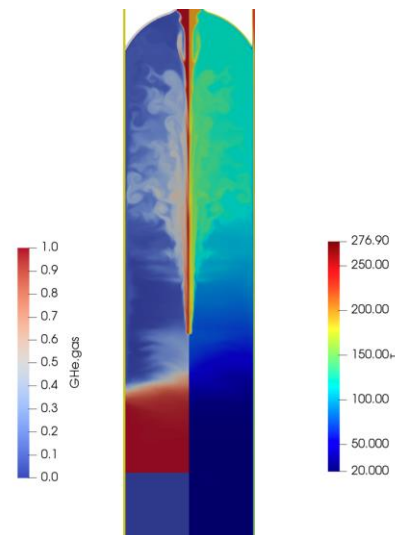


Figure 6: CFD simulation of the LH2 tank, indicating pressure gas fraction and temperature distribution

Detailed investigations concerning the fluid motion and the heat and mass transfer are supported by simulations with a DLR in-house computational fluid dynamics (CFD) software, based on the OpenFOAM framework. With this approach all relevant aspect of propellant management can be analyzed, including different pressurization gas species, heat and mass transfer at the phase boundary, as well as heat transfer to the structure and the external thermal insulation. Example results are visualized in Figure 6.

### 3.3 Approach and Landing System

For vertical landing the CALLISTO vehicle is equipped with a deployable landing gear, which is called the ALS. It is folded during ascent and deploys shortly before touchdown by pressurization of the telescopic primary strut, as can be seen in Figure 7.

In 2021, breadboard models of a single landing leg are built and two main functions have been tested: The deployment and the touchdown.



Figure 7: ALS in folded (left) and deployed (right) configuration

#### 3.3.1 Deployment test campaign

Main goal of the development test campaign is to justify the preliminary design of the complete functional deployment chain, which includes electrical, mechanical and pneumatic functions.

For the deployment test campaign, a conservative step-by-step approach has been applied at DLR's Landing & Mobility Test Facility (LAMA) in Bremen, in order to ensure the structural integrity of the test specimen. First, manual unfolding tests are conducted to ensure the combined kinematic functionality of all moving elements. Then, electrical functions are added and tested. In a last step, the pneumatic components are included to the test setup.

As shown by the yellow lines in Figure 8, a counterweight is attached to the footpad to simulate the aerodynamic drag during descent in the lower atmosphere. This rope spans from the end of the landing leg to the diverter pulley on top of the test stand down to the counterweight. To reduce shock loads, resulting from latching of the telescopic strut, the initial deployments are conducted with a high counterweight, so that the deployment velocity, and hence the latching

energy remains low. For the following test runs, the counter loads are successively reduced, to gradually increase the deployment velocity and stress on the legs.



Figure 8: Landing leg at deployment test stand inside LAMA, left: folded, right: deployed

As a result, it has been shown that the preliminary ALS design is capable to handle the complete deployment functional chain, beginning with deployment initiation by the controller, releasing of the Launch Lock Release Mechanism (LLRM), actuation of the pneumatic valve, and finally the kinematic unfolding including latching in deployed configuration.

Besides the overall success of this campaign and the current ALS design, a few new challenges have been identified. For example, the design and tolerances of the interfaces between primary strut segments can be improved, in order to reduce friction and increase stiffness of the interfaces, hence to ensure product durability and deployment performance. Test predictions are challenging as well, but based on the collected data the supporting multi-body simulation can now be improved to better support the upcoming qualification test campaign.

#### 3.3.2 Touchdown test campaign

To test the damping behavior and the structural integrity of the landing leg, dedicated touchdown tests have also been performed. As can be seen in Figure 9, the leg is attached here to a sliding carriage (orange) on a drop tower which falls along a rail track (blue).

For these tests an upgraded model of the landing leg with carbon tubes and titanium interfaces is used to get representative results of the flight-like structure. For the individual tests the sledge is lifted up to the planned drop height and an electro-magnet at the top triggers the release. The sledge can be turned by several degrees to the front and to the side to simulated inclined landing conditions. Acceleration-, force-, and laser-sensors are measuring the structural health of the specimen.



Figure 9: Single Leg Teststand inside LAMA

In summary, the overall test campaign can be declared successful. High quality data has been received for each test run and the leg withstood all touchdown conditions. However, the forces at the interfaces were higher, while the damping of the used honeycomb cartridges was lower than expected. Also, good experience about the mountability and accessibility of some critical parts of the landing leg could be gathered. These findings will be used to improve the leg design for the next campaign, which may include a slight change of the shock absorber design.

The next activity for the ALS development foresees, amongst others, further deployment and drop test campaigns, as well as environmental tests including vibrational and thermal verifications. With each iteration the leg design improves further to ensure the flight worthiness of the final flight model.

### 3.4 Guidance and Control System

CALLISTO's Guidance and Control System foresees a modular architecture to feature dedicated control laws for each flight phase, which are the ascent, boostback, aerodynamic and landing phases. This choice allows to design guidance and control strategies specifically tailored for the different flight regimes and configurations that CALLISTO will experience throughout the mission. For example, during the ascent and the landing phase it is possible to rely on the FCS/R and FCS/V actuators, which this is not the case in the aerodynamic phase where the engine, and therefore the FCS/V, is off while the FCS/A is deployed.

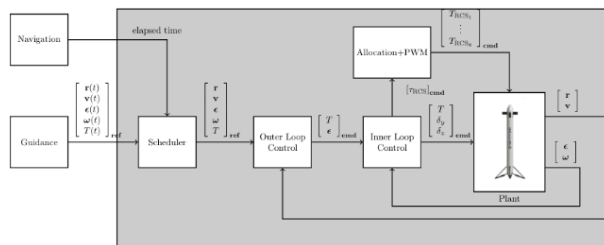


Figure 10: General control scheme for CALLISTO

For individual control design the use of  $H_\infty$  control techniques allows to include and model uncertainties to be counteracted by the feedback control loop to ensure that the trajectory is accurately tracked [5][6]. A scheme representing the general control architecture for CALLISTO is depicted in Figure 10. Note that, due to the aforementioned peculiarities of the different phases, not every element will be present in each phase.

One key aspect of CALLISTO is the capability to generate onboard guidance solutions reflecting off-nominal, inflight conditions. Once again, the different phases will adopt different strategies for this task. For example, during the landing phase the system will rely on sequential convex algorithms, whose preliminary results show encouraging capabilities of being used for such an ambitious mission [7]. An example of the generated landing trajectory is depicted in Figure 11. It shows the body axes of the CALLISTO demonstrator while performing the pinpoint landing maneuver (left figure). Note that the algorithm is capable to incorporate the trimming of the vehicle in the onboard generation of an optimal trajectory (right figure), ensuring that the proposed 3-DoF guidance subsystem will compute 6-DoF feasible trajectories.

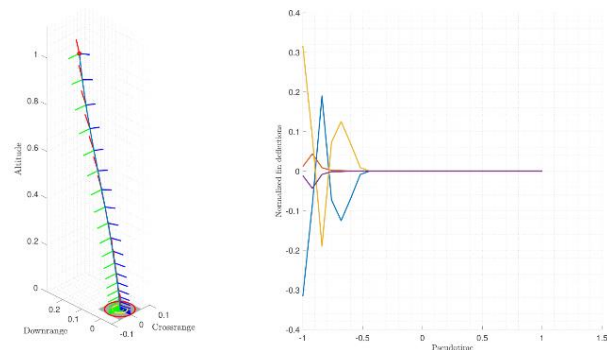


Figure 11: Example of landing trajectory and corresponding normalized fin deflections.

### 3.5 Hybrid Navigation System

The Hybrid Navigation System (HNS) is developed to implement an advanced navigation approach devoted to reusable space transportation systems. It is responsible for providing estimates of the vehicle state, such as position, velocity, attitude and angular rates, to the guidance and control functions and to provide the authoritative basis for time synchronization onboard the vehicle. The term *hybrid navigation* refers to the combination of high-frequency inertial measurements with lower frequency data of other sensors by means of data fusion. In the case of CALLISTO, GNSS receivers and radar altimeters are used as additional sensors, while for other applications sensors like laser altimeters, Sun sensors or star trackers can be incorporated as well. Those sensors provide absolute measurements of

external physical quantities to periodically correct for estimation errors resulting from the integration drift of pure inertial sensor data. This approach allows for lowering the performance requirements on the Inertial Measurement Unit (IMU) while still achieving a superior medium- and long-term navigation accuracy compared to purely inertial systems.

The core avionics of the HNS is being developed in the frame of the ReFEx project, a DLR-internal project for the development of a Vertical Take-Off, Horizontal Landing (VTHL) technology demonstrator [8]. For CALLISTO, the HNS core avionics, software, development methodology and tools are kept identical as much as possible in order to exploit the most possible synergy between both projects, whereas adaptations to the sensor suite, algorithms, and alignment strategy are introduced to consider CALLISTO's mission needs.

The preliminary design phase of the HNS has been successfully concluded in September 2021 with the involvement of independent reviewers from industry. In this course, all requirements imposed from system and mission side have been defined and consolidated with the project stakeholders into a comprehensive requirement specification.

On this basis, several studies and trade-offs for establishing a baseline HNS architecture have been performed, which led to the selection of an advanced multi-constellation, multi-frequency GNSS subsystem using the Galileo and GPS constellations. An additional GNSS ground reference station close to the landing pad enables the use of code-based differential GNSS correction techniques, as well as an RTK-based approach for more accurately determination of the flight altitude above the landing pad in the final flight phase. In parallel, a second approach to determine the flight altitude is developed and evaluated which is based on a radar altimeter system with radar reflectors close to the landing pad.

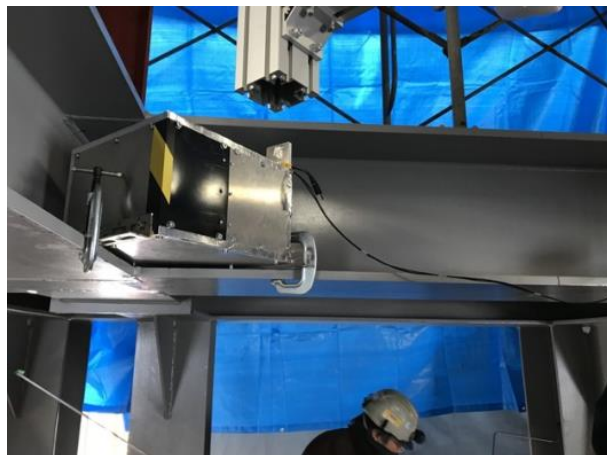


Figure 12: Radar altimeter prototype integrated into the engine test stand.

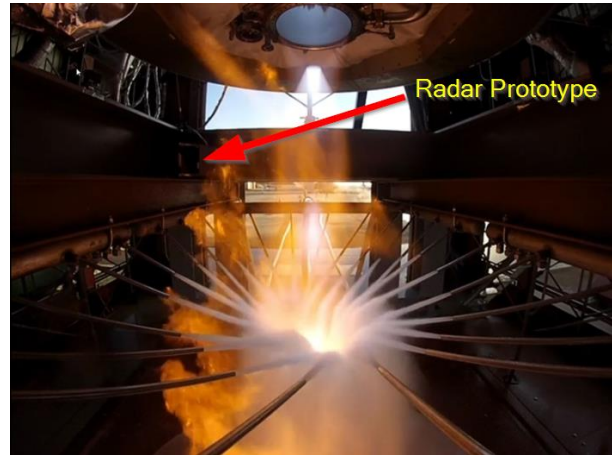


Figure 13: Measurements with the radar altimeter prototype during engine static firing test in NTC

For the radar altimeter system, concerns have been raised related to the possible interactions of the radar signals with the engine plume. To investigate this risk, a radar prototype has been built and tested at JAXA's Noshiro Rocket Testing Center (NTC) during a static firing test of the engine. As can be seen in Figure 12 and Figure 13, the radar prototype and a radar reflector were integrated into the engine test stand so that the radar signals had to pass back and forth directly through the engine plume during all phases of engine operation. It was found that there is no significant negative impact on the radar signals due to engine operation and that the radar technology can be used in principle for CALLISTO. A preliminary design of the complete radar altimeter system has been developed subsequently.

On the other hand, there have also been concerns about the robustness of the RTK-based approach as this technology has not been used in similar applications before. A thorough modeling and simulation campaign as well as a series of laboratory hardware tests revealed that this approach is more robust than initially supposed. Since a GNSS ground reference station is already foreseen, the effort for implementing the RTK-based flight altitude estimation is comparatively low in contrast to the custom development of a radar altimeter system and its associated complexity. At the beginning of the detailed design phase, a decision whether to implement the radar altimeter system or the RTK-based approach will be made.

The sensor suite considerations were accompanied by detailed modeling and simulation of the sensors and navigation algorithms to assess the performance in various system configurations. In order to meet the demanding attitude estimation accuracy requirements, it has been found that the initial attitude knowledge during HNS initialization before launch has a significant impact. In consequence, a concept for performing an external alignment based on optical measurements has

been developed and evaluated to improve the attitude estimation accuracy during the ascent phase. However, refinement of the navigation performance requirements is ongoing with the potential to relax the requirements in a way that an external alignment may not be needed.

Another major challenge which could not be solved yet and which still has to be tackled both on subsystem and overall system side are the relatively high vibrations under which the inertial sensors have to operate. Concepts for locally reducing the vibration levels have been investigated and it became clear that such local measures alone are not sufficient to bring the vibrations into an acceptable range. The sensor behavior under vibration has been modeled to the extent possible based on available manufacturer specifications. As soon as a lab prototype of the IMU is available, a dedicated characterization campaign will be performed in order to refine the sensor models.

With the successful completion of the HNS Preliminary Design Review (PDR), the development transitions now into the detailed design phase, during which a complete engineering model of the HNS is being built while the main work on the simulations and software is about to be concluded.

### 3.6 Aerodynamic Control System (FCS/A)

The purpose of the FCS/A is to ensure aerodynamic stability and controllability of the CALLISTO vehicle during descent flight, while producing only minimal aerodynamic drag during ascent. As shown in Figure 14, the design consists four deployable aerosurfaces, each having a dedicated electromechanical actuator and a deployment hinge mechanism, as well as an LLRM interface with the LOX Tank. Not depicted is the FCS/A controller box inside the VEB.

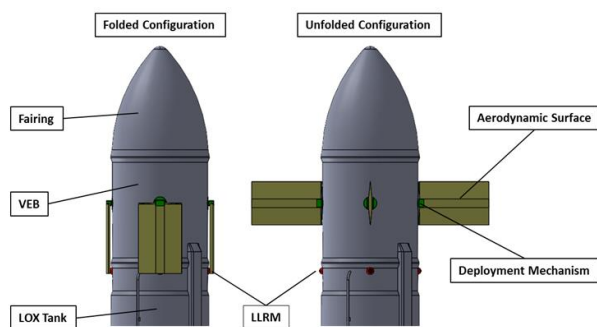


Figure 14: FCS/A in ascent (left) and descent (right) configuration

As the FCS/A design has successfully passed PDR stage, prototype models for several critical components have been built and tested. Besides others, these tests included electromagnetic compatibility (EMC) and depressurization tests of the power supply, as well as mechanical life cycle tests of the flexible harness.

The internal power supply is on one hand responsible to convert the 28 V DC board net voltage of CALLISTO to 48 V DC for actuators supply. On the other hand, it needs to limit the peak power demand on the board net, which is realized by DC link capacitors used as temporary energy buffers. A rendering of the power supply board is shown in Figure 15.

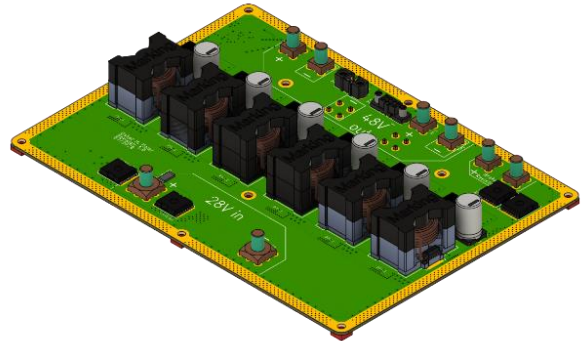


Figure 15: Computer-rendered graphics of FCS/A internal power supply

Due to the high frequent switching of large voltages and currents, EMC is a major concern for the power supply board. However, first prototype tests have shown the compliance to the EMC requirements of CALLISTO. Furthermore, the robustness of the large electrolytic capacitors against rapid de- and repressurization has been tested in a vacuum chamber. In this setup a batch of capacitors has been cycled between maximum and minimum expected pressure of the most demanding flight profile for a life cycle well beyond the envisaged 10 flights. After each cycle the capacitors are checked for physical changes and their capacity and equivalent series resistance (ESR) is measured. No degradation or failure could be identified in this campaign.

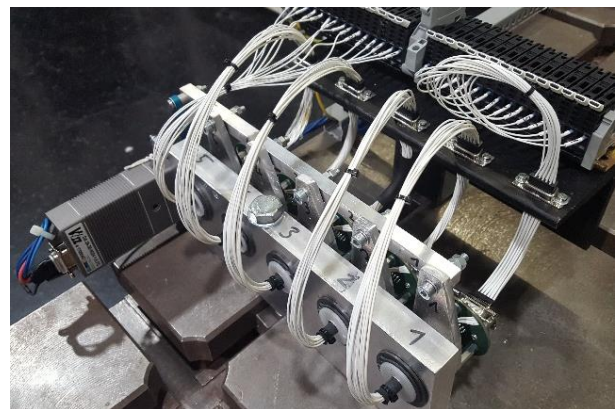


Figure 16: Test setup for flexible harness life time test

For the flexible harness, which connects sensors in the fins to the vehicle avionics, an accelerated life time test has been performed as shown in Figure 16. Here,



different configurations of the harness have been tested to select the most suitable for the actuator design.

Further hardware tests are currently ongoing, including functional test of the hinge mechanism and vibration tests of the LLRM. Apart from testing, extensive Finite Element Model (FEM) analyses have supported the confidence in the developed design. Mechanical and thermal analysis of the structural components, as well as transient thermal simulations of the full controller under load have been performed and used for optimization.

In order to ensure the absence of harmful aeroservo-elastic coupling, such as flutter, numerical studies have been performed to investigate the dynamic stability behavior of the FCS/A in unfolded configuration during descent. For this purpose, a condensed FEM of the aerosurface is used in conjunction with the actuator and VEB interface stiffness matrices to obtain the structural dynamic properties similar to a wind tunnel setup. The required unsteady aerodynamic matrices are computed for several Mach numbers and reduced frequencies by the Doublet Lattice Method (DLM) implemented within the MATLAB-based tool VARLOADS [9][10]. Although the DLM provides good computational efficiency and quality for typical aircraft geometries, it is applicable only for subsonic compressible attached flow which limits the Mach range of the examined flight envelope. Subsequently, the p-method [11] has been applied to assess the dynamic stability of the FCS/A for suitable Mach number and altitude combinations. The results indicate that, within the subsonic descent flight envelope and validity of the applied methods, dynamic instabilities such as flutter cannot be detected. The influence of the full vehicle structural dynamics and the actuator dynamics on the stability behavior under free flight conditions is currently under investigation.

### 3.7 Reaction Control System (FCS/R)

The FCS/R is another key component of the flight control system of CALLISTO. Its primary functions are to perform:

- Roll control during engine “ON” phases;
- 3-axis control during engine “OFF” phases.

A specific property of the CALLISTO high energy flights is that the MECO occurs at relative low altitudes within the atmosphere, thus creating significant aerodynamic torque during any maneuver. As a result, and since the main propulsion system is “OFF” during these phases, significant torque control capability needs to be provided by the FCS/R only.

The baselined FCS/R architecture features eight H<sub>2</sub>O<sub>2</sub> thrusters, each providing 200N thrust in vacuum conditions. The system, including its propellant tank, is located inside the VEB Module near the top of the Vehicle to maximize control lever arm of the thrusters. The general layout of the system is given in Figure 17.

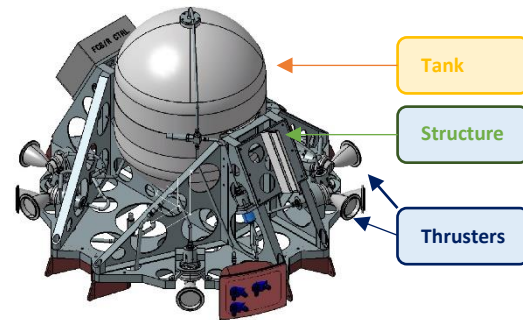


Figure 17: FCS/R notional layout (courtesy of Nammo)

### 3.8 Aerodynamics and Aerothermodynamics

The aerodynamic and aerothermodynamic evaluation of the CALLISTO vehicle is under DLR responsibility. This includes the aeroshape definition and optimization, performance assessment, estimation of aerodynamic and aerothermal loads, as well as uncertainty analysis before and after the flights. For this purpose, various studies using CFD and wind tunnel experiments were already conducted in early project stages [12][13].

Main challenges for the characterization of CALLISTO aerodynamics are on one hand the extensive number of possible configurations and conditions, which include un-/deployed legs and fins, various engine operation levels including thrust vectoring, as well as large ranges for angles of attack and roll angles with a slightly asymmetric aeroshape, on the other hand the integration of the multiple data sources into consistent system engineering databases.

In order to satisfy the technical needs for system development, the aerodynamic analyses are based on:

- Wind tunnel tests (WTT) for different configurations and conditions at the
  - DLR Trisonic Wind Tunnel (TMK) in Cologne [6], the
  - DNW High-Speed Tunnel (HST) in Amsterdam, and the
  - CSTB wind tunnels in Nantes (conducted by CNES).
- Extensive number of low-resolution CFD calculations for all configurations and conditions, as well as
- Moderate number of high-resolution CFD calculations for all configurations and conditions, including some WTT setups.

Based on this data, multiple aerodynamic databases (AEDB) and aerothermal databases (ATDB) have been compiled which provide application programming interfaces for external system analyses, such as guidance and control design or thermal analysis. Besides from the database generation, key progresses have been made in successful conclusion of wind tunnel test campaigns, progress in wind tunnel CFD calculations

and uncertainty estimation, as well as local aerothermal analysis.

In October 2020 an extensive WTT campaign at the HST was conducted in order to address the vehicle design progress. As shown in Figure 18, a large-scale model (1:10) with a detailed replication of the outer shape was manufactured and tested in this setup to reproduce local aerodynamic effects. This campaign is therefore complementary to previously performed WTT experiments at the TMK [12], which tested a simplified CALLISTO aeroshape at 1:35 scale.



Figure 18: CALLISTO 1:10 scale model with unfolded fins mounted in the HST test setup

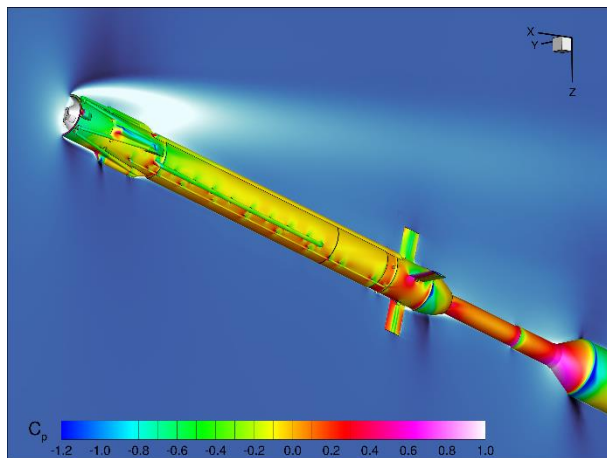


Figure 19: Simulated surface pressure coefficient for the wind tunnel test at  $M=0.9$  and  $AoA=195^\circ$ .

Focus of the test campaign was on precise measurement of force and moment coefficients for all relevant flight conditions. These results were used to verify and improve the accuracy of the AEDB and to support the uncertainty assessment. Additionally, flush mounted pressure sensors in the base region and near the fins were used to acquire stationary and in-stationary pressure measurements which are used to validate the structural loads during flight. In total nearly 600 angle of attack and roll polars were generated for Mach

numbers between 0.2 and 1.3, and for folded and unfolded fins with different deflections. A variation of Reynolds number for certain conditions also made comparison with TMK data possible.

To evaluate scaling effects and the influence of the model support, dedicated WTT conditions have been simulated using the DLR in-house CFD code TAU [14]. For example, Figure 19 shows the surface pressure distribution for an HST simulation at a free stream Mach number of 0.9 and an angle of attack of  $195^\circ$ . As the AEDB is mainly based on CFD simulations, the WTT results together with the numerical rebuilding of these tests allow the quantification of uncertainties in the datasets. These estimations have also been supported by analysis of different turbulence models which have a significant effect on the simulated loads.

For the aerothermodynamic analyses a focus was on the creation of the ATDB which provides heat fluxes onto different parts of the vehicle. Based on a combination of 2D and 3D CFD calculations a database dependent on Mach number, air density and angle of attack between 160 deg and 180 deg is generated, which covers the full powered return trajectory. The conceptual database structure is shown in Figure 20. Further 3D simulations were conducted to quantify influences of roll angle, engine thrust level and landing legs angle. Based on these results, improved thermal zoning for the vehicle components have been proposed in consultation with engineering teams to create sensible thermal requirements for the detailed design phase.

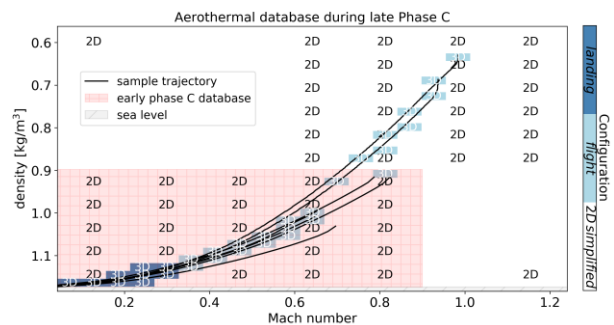


Figure 20: Aerothermal database (ATDB) for powered return flight with full thrust.

Local aerothermal analysis is especially important for the thermal protection of structures immersed in the hot engine exhaust jet, like the ALS. Here, a clear influence of the engine thrust level onto the heat flux distribution on the landing legs could be observed. The upper two simulations in Figure 21 show the influence of different Mach numbers on the heat flux to the legs. At  $Ma=0.5$  the struts of the legs receive a high heat flux due to the hot exhaust plume being pushed towards them. This effect is weaker for  $Ma=0.23$  below, even though the foot pads receive a higher heat flux due to a

less compact plume. For a lower thrust level of 40%, shown at the bottom of Figure 21, the flow structure at  $Ma=0.23$  is more similar to the  $Ma=0.5$ , thrust=100% case, but with an overall lower heat flux.

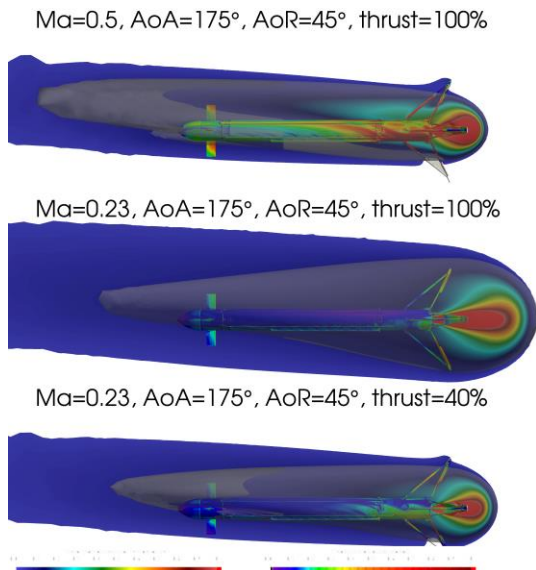


Figure 21: 2D slice of temperature, isosurface of 99% exhaust species, Surface: heat flux.

Overall good progress has been made in the aerodynamic and aerothermal characterization of the CALLISTO vehicle using a multitude of wind tunnel experiments and detailed CFD analyses. The next steps include delta aerodynamics for the final aeroshape, uncertainty consolidation and final data validation.

### 3.9 Fairing

The primary function of the Fairing is to protect the top of the CALLISTO demonstrator from the external aerodynamic flow, particularly during the ascent flight. Besides that, some equipment is accommodated inside the Module: the GNSS Antenna, as well as elements of the FNS and the scientific instrumentation. A side view can be seen in Figure 22.

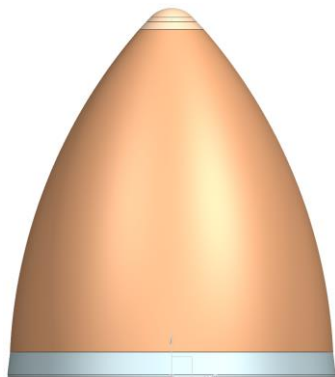


Figure 22: Side view of the Fairing Module

The current structural design is based on mechanical analyses with refined material properties for the ogive CFRP-sandwich main body. The underlying database, which features common CFRP values and separate data sheets for fibers and resins, has been extended with material characterization tests of in-house cured CFRP specimens to fit the final product in material and process. As a full material qualification is very time and cost intensive, a shortened campaign of tension and compression tests at room and elevated temperatures was carried out. In that way, a confirmation and correction of the material parameters was possible with relatively few means.

One major design driver for the fairing is the heat load from the engine plume during the landing maneuver, as it exceeds the thermal capabilities of the CFRP structure. This challenge is solved with a reusable thermal protection system (TPS) on top of the load carrying structure. Therefore, an iterative process of combined analytical estimations and numerical calculations has been established to fit the aerothermal boundary conditions with a sound temperature distribution on the structure.

For range safety reasons, parts of the FNS are implemented inside the fairing. This includes a range of pyrotechnic devices which are placed on the inside wall of the CFRP sandwich ogive. The attachment is realized with specially designed GFRP clips to allow an easy installation and safe accommodation. A proof of concept will be done via shaker tests.

As the vehicle may descend through humid air, condensation inside the fairing should be avoided. In this context special attention is paid on the GNSS antenna, which may show degraded performance under water deposition. To face this challenge, the very tip of the vehicle is designed as a closed chamber with check valves. They allow the dry air to flow out during ascent flight, but prevent the humid air from entering the antenna cavity. This implies the presence of an artificially under-pressure during descent, which need to be sustained by the curved radome. A qualification of the valves is planned via in-house shaker tests.

### 3.10 Vehicle Equipment Bay

The VEB Module is located between the LOX Tank Module and the Nose Fairing Module. As shown in Figure 23 it is composed of the following main components:

- the VEB structure, which supports all the other products and which mainly ensures the load transmission between the Nose Fairing Module and the LOX Tank Module;
- the cable duct covers, ensuring the protection of the electrical and fluidic interfaces with the bottom part of the vehicle.

- the FCS/A, which provides the flight control means during reentry phase
- the FCS/R, which provides the flight control means during atmospheric flight in ascent phase
- the avionics products, dedicated to on-board data management, power supply, control of propulsion system, telemetry and telecommand, flight neutralization and hybrid navigation.

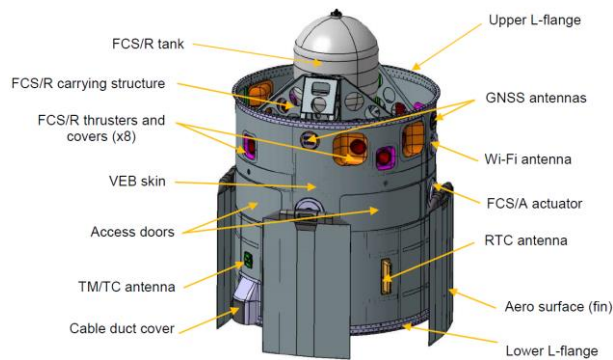


Figure 23: VEB Module external view

The structural design of the VEB consists of stringers and frames covered by a thin cylindrical skin, which implements a classical aluminum lightweight structure. This design, which is depicted in Figure 24, was investigated in more detail during a trade-off study that compared different design approaches [15]. The trade-off compared accommodation options on unit platforms versus structural elements for unit support, as well as a pure cylinder with thickness adjusted walls versus the classical stringer and frame design. It turned out that the classical stiffened design with structural unit supports is far superior, even though it is slightly less flexible in accommodation options.

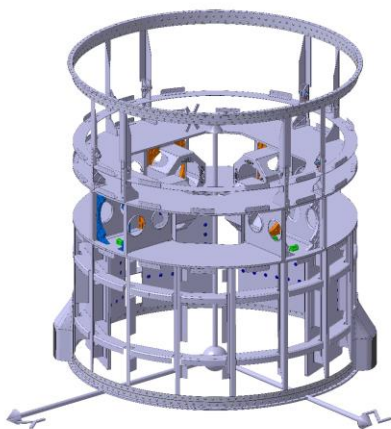


Figure 24: Open view of the VEB structure without skin

A major design challenge is the load introduction for the FCS/A and FCS/R. Therefore, the VEB is locally stiffened by a frame and web configuration, the so-

called inertia box. This box bears the actuators of the FCS/A between and the support structure of the FCS/R on top of two aluminum sandwich frames, connected by eight vertical webs. The electrical power supplies are also placed inside the inertia box to be accessible from outside through doors.

Further equipment is located in the lower part of the VEB. Therefore, vertical support plates are mounted onto the stringers and frames. In case of equipment's interface deviations, these support plates give the flexibility to be replaced instead of remanufacturing structural hard points. At the upper and lower end of the VEB L-flanges serve as interfaces to the fairing and the LOX tank.

### 3.11 Flight Neutralization System

Since the CALLISTO vehicle is being operated from the CSG on French territory, it needs to comply with the French regulations related to launch activities either on ground or during flights. According to its very specific mission profile compared to legacy ELVs, particularly due the high verticality of the trajectory, flight safety studies showed the stringent necessity for neutralization capability of the vehicle. The implemented FNS combines:

- A localization function, featuring both Radar transponder (ground-based localization) and on-board GNSS (autonomous localization)
- A flight termination function, which makes uses several pyro-cord devices along the vehicle in order to be activated in off-nominal scenarios.

The FNS layout benefits from two cable ducts running along the vehicle wall, in order to maintain physical segregation of the termination devices and thus to mitigate risks for single points of failure. The development of the FNS relies both on existing technologies and on new developments, such as the pyro-cords initiators and autonomous localization [1].

### 3.12 Conditioning System

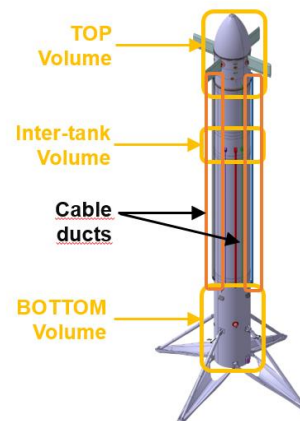


Figure 25: Closed volumes inside CALLISTO vehicle

Primary function of the Conditioning System is to manage the environmental conditions, such as temperature, pressure and species concentration, inside the closed volumes of the vehicle, since they are housing sensitive avionics components. An overview of these closed volumes is sketched in Figure 25.

During ground phases, particularly until lift-off and after reconnection to the GSE on the landing pad, the conditioning system is an active system which provides temperature controlled GN2 from the ground segment. As shown in Figure 26 the main GN2 distribution line is located in one of the two cable ducts to condition the top, inter-tank and bottom volumes, and the cable duct itself. The other cable duct is conditioned through the top volume. The flow rate into each closed volume can be further controlled and fine-tuned via secondary pipes, nozzles and diffusers, while avoiding any moving parts.

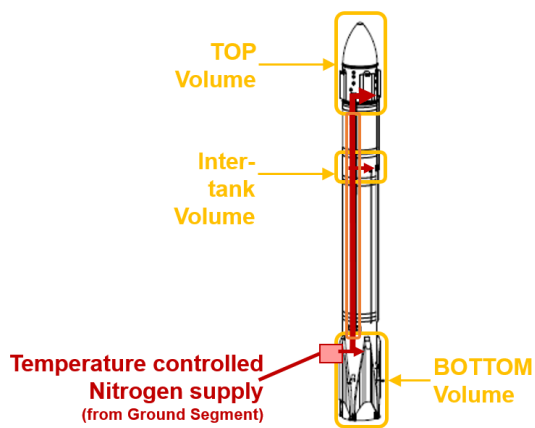


Figure 26: GN2 distribution during ground phases

During flight, the conditioning system is passive and relies on a set of vent holes, specifically designed to:

- 1) Allow balancing between the inner and outer pressure to limit mechanical loads on the load-carrying structures,
- 2) Manage related de- and repressurization rates in the closed volumes in dependence of the ambient pressure at different altitudes,
- 3) Limit ingesting rain and foreign objects with scoops and grid behind the vent ports.

Although the system is fully passive during flight, the vent holes design allows adaptation of the flow section from one flight to another, if necessary.

### 3.13 Ground Segment

The primary functions of the Ground Segment are:

- To prepare the vehicle for flight,
- To provide installations for flight operations: lift-off, recovery and operations in between, such as vehicle tracking,

- To inspect and maintain the vehicle between two flights.

Compared to other launch systems operated at CSG, CALLISTO is a very unique system, since:

- Three partners share duties for vehicle preparation, flights and maintenance operations,
- Small and light vehicle versus legacy launchers,
- Period of operations is less than one year versus decades for commercial launchers.

Due to the physical properties of the CALLISTO vehicle, such as size, mass, and propellant species, and the characteristics of the demonstrator program itself, CALLISTO relies on existing installations and GSE.

Concentrating on installations, vehicle preparation including Maintenance & Repair Operations (M&RO) will be completed in a building dated back to the seventies that is retrofitted for CALLISTO: the Vehicle Preparation Hall (VPH), which was initially used for the Diamant rocket program. The VPH is the large-sized building in Figure 27 retrofitted from the assembly hall nearby the moving launch tower. Other installations, like the launch tower itself, are either already discarded or will remain on site.

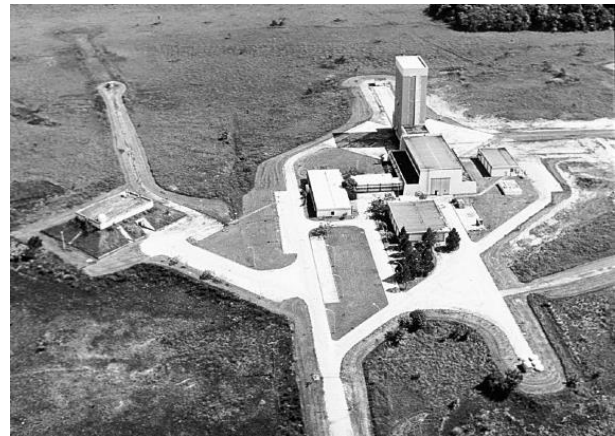


Figure 27: Diamant rocket launch complex

Focusing on the fluidic GSE, the propellant farm is located close to the VPH for both cryogenic propellants and two mobile trailers. Other fluids needed for ground and flight operations are also located nearby: gaseous helium for the vehicle propulsion system, gaseous compressed air for ground operations like cleaning and testing, as well as H<sub>2</sub>O<sub>2</sub> as FCS/R propellant. There is one exception for gaseous nitrogen used by the conditioning system, which is supplied via devoted piping network.

For the mechanical GSE, existing or rented material, such as forklifts, trailers, mobile cranes and cherry-pickers, are combined with material specifically developed for CALLISTO. The latter includes (i) hoisting devices, (ii) the lift-off table and (iii) a pair of all-moving cryogenic arms, as shown in Figure 28, to

clear the lift-off area ahead of take-off. Additionally, there is a devoted robot to provide safety-critical functions on the landing pad after flight: gaseous helium and nitrogen supply, electrical power distribution and wired data communications. This is also used for disconnection ahead of take-off at the lift-off pad.

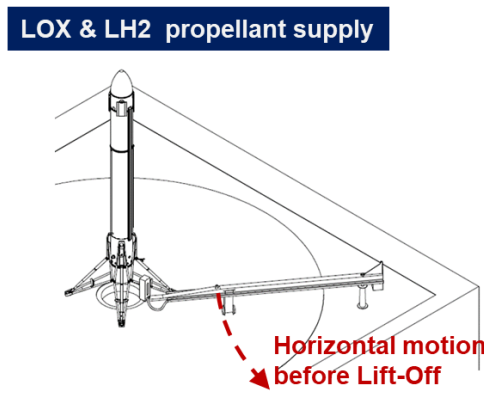


Figure 28: Propellant supply on lift-off pad via all-moving arms

Last but not least, the CALLISTO Launch Complex includes also the Control/Command Center and its electrical GSE, which is operated jointly by the project partners. It serves as the single control & command tool during flight preparation including M&RO, ahead or after flight, and on any site: VPH, Lift-Off Pad or Landing Zone. The Control/Command Center itself is located in a remote area distant from Diamant site.

Aside from local site-specific functions, some are provided globally to all CALLISTO sites:

- A common data management system,
- A single control & command room,
- A control & command bench to manage the different processes,
- A network to link either the control command to one single site or between different sites.

Direct interfaces to Launch Range services are also provided, such as the data link in between the Telecommand/Telemetry station network and the Control/Command Center.

Regarding the maturity of the Ground Segment, all PDRs have been completed successfully, which paves the way to contract the different work packages for Launch Complex preparation, to become operational in 2023. In parallel, time critical civil engineering activities has already started, such as cleanup of the Diamant site or setup of the ancillary network.

#### 4. Development Roadmap and Outlook

After successful completion of the Preliminary Design Reviews (PDR), the subsystems enter the detailed design phase, which is concluded with dedicated Critical Design Reviews (CDR). During this

phase, the design has to be refined and all identified problems have to be addressed and solved, in order to move forward to the qualification of the subsystems in the next step. Dedicated qualification tests are necessary to verify initial analyses and to demonstrate for instance the ability of the subsystems to sustain the critical load cases.

In parallel to the development of subsystems, test campaigns at system level support the verification process: the avionic components are tested in a dedicated Avionic Validation Facility (AVF) in France. Hot firing tests in Japan support the qualification of the bottom module components in an assembled configuration.

The successfully completed qualification phase leads to the start of flight hardware manufacturing. Then, final acceptance tests on the flight models allow the authorization for the shipment to French Guiana, where the final vehicle integration takes place. After a combined tests phase, the 6-months flight campaign begins, covering up to 10 flights in total. Here, an incremental approach is followed, going from low-risk to high-energy flights. Each flight is authorized by a Flight Readiness Review (FRR).

#### 5. Conclusions

As shown in the previous chapters, significant progress has been made in the development of key technologies for the CALLISTO demonstrator. Detailed analyses and representative breadboard tests on subsystem level have supported the feasibility assessment of the chosen design. While the obtained results are used to further optimize the design, no technical show stopper could be identified so far.

Up to now, the vehicle, the ground segment and most subsystems have successfully passed PDR stage. With regard to the development logic, this allows to continue the detailed design phase and successively move on to the qualification campaigns. CNES, JAXA and DLR are striving to keep a good pace in this already fruitful cooperation for a first launch in 2024.

#### References

- [1] S. Guedron, S. Ishimoto, E. Dumont et al., CALLISTO Demonstrator: Focus on system aspects, 71st International Astronautical Congress (IAC), IAC-20-D2.6.1, Dubai, UAE, 2020, [link](#).
- [2] E. Dumont et al., CALLISTO: A Demonstrator for Reusable Launcher Key Technologies, Transactions of the Japan Society for Aeronautical and Space Sciences, Aerospace Technology Japan, 2021, Volume 19, Issue 1, pp. 106-115, [link](#).
- [3] DLR, CALLISTO, 05 October 2020, [link](#) (accessed 17.09.2021).
- [4] S. Nonaka, T. Ito, and Y. Inatani, Technology Demonstrations and System Design for Reusable

Rocket Flight Experiment, 68th International Astronautical Congress (IAC), IAC-17-D2.5.4, Adelaide, Australia, 2017.

- [5] J. A. Macés, M. Sagliano, A. Heidecker, D. Seelbinder, M. Schlotterer, S. Farí, S. Theil, S. Woicke, E. Dumont, Ascent Flight Control System for Reusable Launch Vehicles: Full-Order and Structured  $H_\infty$  Designs, 11th International ESA GNC Conference, May 2021, [link](#) (accessed 14.09.21).
- [6] M. Sagliano, T. Tsukamoto, A. Heidecker, J. A. Macés, S. Farí, M. Schlotterer, S. Woicke, D. Seelbinder, S. Ishimoto, E. Dumont, Robust Control for Reusable Rockets via Structured  $H_\infty$  Synthesis, 11th International ESA GNC Conference, May 2021, [link](#) (accessed 14.09.21).
- [7] M. Sagliano, A. Heidecker, J. A. Macés, S. Farí, M. Schlotterer, S. Woicke, D. Seelbinder, E. Dumont, Onboard Guidance for Reusable Rockets: Aerodynamic Descent and Powered Landing, AIAA Scitech 2021 Forum, January 2021, [link](#) (accessed 14.09.21).
- [8] W. Bauer, P. Rickmers et al., DLR Reusability Flight Experiment ReFEx, Acta Astronautica, 2019, Volume 168, pp. 57-68, [link](#).
- [9] J. Hofstee, T. Kier, C. Cerulli, G. Looye, A Variable, Fully Flexible Dynamic Response Tool for Special Investigations (VARLOADS), International Forum on Aeroelasticity and Structural Dynamics (IFASD), 2003.
- [10] T. M. Kier and G. H. N. Looye, Unifying Manoeuvre and Gust Loads Analysis Models, International Forum on Aeroelasticity and Structural Dynamics (IFASD), 2009.
- [11] R. J. Zwaan, Aeroelasticity of Aircraft, 1999.
- [12] A. Marwege, J. Riehmer, J. Klevanski, A. Gülhan, T. Ecker, B. Reimann, E. Dumont, First Wind Tunnel Data of CALLISTO Reusable VTVL Launcher First Stage Demonstrator, EUCASS 2019 Conference, Madrid, Spain, 1 – 4 July 2019, [link](#).
- [13] J. Klevanski, T. Ecker, J. Riehmer, B. Reimann, E. Dumont, C. Chavagnac, Aerodynamic Studies in Preparation for CALLISTO - Reusable VTVL Launcher First Stage Demonstrator, 9th International Astronautical Congress (IAC), IAC-18-D2.6.3, Bremen, Germany, 2018, [link](#).
- [14] D. Schwammborn et al., The DLR TAU-Code: Recent Applications in Research and Industry. ECCOMAS CFD 2006 Conference, Delft, The Netherlands, 2006.
- [15] O. Mierheim, L. Heinrich, T. Glaser et al., A Trade-Off Study for the Structure of the CALLISTO Vehicle Equipment Bay, 16th ECSSMET, online, 2021, 23-26 March, [link](#).